Advances in Nano Research, *Vol. 11, No. 4 (2021) 347-359*
https://doi.org/10.12989/anr.2021.11.4.347

New state-space approach to dynamic analysis of porous FG beam under different boundary conditions

Youcef Tlidji[1], Rabia Benferhat[1,2], Luan Cong Trinh[3], Hassaine Daouadji Tahar*[1,2] and Tounsi Abdelouahed[4,5,6]

[1]*Department of Civil Engineering, University of Tiaret, Algeria*
[2]*Laboratory of Geomatics and Sustainable Development, University of Tiaret, Algeria*
[3]*Faculty of Civil Engineering and Applied Mechanics, University of Technical Education Ho Chi Minh City, Viet Nam*
[4]*YFL (Yonsei Frontier Lab), Yonsei University, Seoul, Korea*
[5]*Department of Civil and Environmental Engineering, King Fahd University of Petroleum & Minerals, 31261 Dhahran, Eastern Province, Saudi Arabia*
[6]*Material and Hydrology Laboratory, University of Sidi Bel Abbes, Civil Engineering Department, Algeria*

(*Received April 24, 2021, Revised August 4, 2021, Accepted August 7, 2021*)

Abstract. This paper investigates dynamic behavior of porous functionally graded beams under various boundary conditions using State-space approach. The material parameters of FG beams change continuously along the thickness direction according to the power-law function (PFGM) or sigmoid function (SFGM). The porous FG beams are assumed to have even and uneven distributions of porosities over the beam cross-section. The classical beam theory, first-order and higher-order shear deformation theories are employed to consider beams of various boundary conditions. Hamilton's principle are employed for derivation of the equations of motion. Fundamental frequencies are calculated numerically for different boundary conditions, gradient index, volume fraction of porosity, distribution shape of porosity, and span-to-depth ratios. The results show that the variation of the distribution shape of porosity has an effect on the fundamental frequencies.
Keywords: dynamic analysis; FG beams; porosity; state-space approach

1. Introduction

Functionally graded material is a category of composites introduced by Japanese material scientists, which the properties vary continuously along a certain direction. The material gradation function's continuity results in overcoming the stress concentrations and delamination disadvantages in laminates. Due to their superior performance and the increasing demand for their characteristics, functionally graded materials' applications have been increasing in various modern industries like aeronautics, thermo-generators, industrial constructions, civil infrastructure, defense, nuclear reactors, mining, nanostructures, and biosensors. Consequently, the accurate prediction of the FGM structures behavior under various loading conditions is important for the design considerations.

The gradient elasticity theory states that materials should be considered as atoms with higher-order deformation mechanism at small scale rather than modeled just as collections of points, and the stress must consider additional strain gradient terms. Yang *et al*. (2002) modified the gradient elasticity theory. The modified gradient elasticity theory states strain energy density must be considered as a function of both strain tensor conju-gated with stress tensor and curvature tensor conjugated with couple stress tensor. By using the modified gradient elasticity theory, Reddy (2011) developed Euler–Bernoulli and Timoshenko beams models for bending, vibration and buckling of FG beams. Simsek and Reddy (2013) presented a unified beam theory that contains various higher order beam theories as well as the Euler–Bernoulli and Timoshenko beam theory for the static bending and free vibration FG microbeams based on modified couple stress theory. Based on the Euler-Bernoulli beam theory, the vibration responses of FGM beams have been widely studied by different approaches. Şimşek and Kocatürk (2009) studied the dynamic response of an FGM simply supported beam under a concentrated moving harmonic load, in which the effects of the material homogeneity, the velocity of the moving harmonic load, and the excitation frequency on the dynamic responses of the beam were discussed. The vibration of structures such as beams is a very important subject to study in particular in civil engineering. Structures behave dynamically when subjected to loads and displacements. Therefore, it is important to analyze the influence of the conditions at the supports on the mechanical behavior of elastic structures in technical studies (Pradhan 2013, Avcar 2019, Abdelhak *et al*. 2016, Benferhat *et al*. 2019, 2021, Sayyad 2018, Ashraf *et al*. 2020, Asrari *et al*. 2020, Behrouz *et al*. 2020, Ghayesh 2018b, 2019c, d, Shariati *et al*. 2020b, Sedighi *et al*. 2014, Benhenni *et al*. 2021, Kablia *et al*. 2020, Abderezak *et al*.

*Corresponding author, Professor,
E-mail: daouadjitahar@gmail.com;
tahar.daouadji@univ-tiaret.dzr

ISSN: 2287-237X (Print), 2287-2388 (Online)

2021, Tlidji *et al*. 2021, Bekki *et al*. 2021, Milad *et al*. 2019). In the framework of the first shear deformation theory or the Timoshenko beam theory, Li (2008) presented analytical solutions for the static bending and free vibration of FGM Timoshenko and Euler-Bernoulli beams (Abdulraoof *et al*. 2020, Ghayesh 2018a, 2019b, Allahkarami, 2020, Anwariningsih 2013, Arefi *et al*. 2020, Emrah *et al*. 2020, Eltaher *et al*. 2020, Ghannadpour *et al*. 2020, Heidari *et al*. 2020, Iakov *et al*. 2020, Koochi *et al*. 2021, Mahesh *et al*. 2020). Huang and Li (2010) also studied the free vibration of axially FGMs with non-uniform cross-sections by using the integration technique to transform the differential governing equations into the Freedom integral equations (Moory-Shirbani *et al*. 2018, Benferhat *et al*. 2020, Le *et al*. 2020, Phung-Van *et al*. 2021, Nazemnezhad and Shokrollahi *et al*. 2020, Tran *et al*. 2020, Abdelhak *et al*. 2021, Benferhat *et al*. 2016, Shariati *et al*. 2020a, Ghayesh 2019a, Sheng *et al*. 2020, Liu *et al*. 2020, Yuan *et al*. 2020, Zhu *et al*. 2020).

In this work, the vibration of micro-beams with functional graduation incorporated which will be studied and analyzed. So we set as the objective of this article is to present a State-space approach to dynamic analysis of porous FG beams under different boundary conditions. The effects of the shear deformation and the parameters influencing the dynamic behavior of beams are discussed in detail. Wherein, it should be stressed that the relationship between the parameters describing the beam vibration and the different boundary parameters will be considered.

2. Mathematical formulation of the present method and solution procedure

2.1 Theoretical formulation

According to the rule of mixture, the effective material properties, *P*, can be expressed as:

$$\boldsymbol{P(z) = P_m V_m + P_c V_c} \tag{1}$$

where P_m, P_c, V_m and V_c are the material properties and the volume fractions of the metal and the ceramic constituents related by

$$\boldsymbol{V_m + V_c = 1} \tag{2a}$$

The effective material properties of the FGM beam is characterized by the power-law form presented by Pradhan *et al*. (2013). The volume fraction of the ceramic constituent and the metal of the beam material is expected to be given by the classical mixing law of FGM materials:

$$\boldsymbol{V(z) = (\frac{1}{2} + \frac{z}{h})^k} \tag{2b}$$

where *k* is the non-negative variable parameter which dictates the material variation profile through the thickness of the beam.

Therefore, from Eqs. (1)-(3), the effective material properties of the FG beam can be expressed as follows:

$$\boldsymbol{P(z) = (P_c - P_m) * V(z) + P_m} \tag{3}$$

On account of a porous FG beam, the rule of mixture should be modified. For even and uneven types distribution shape of porosity, the modified rule of mixture becomes:

Even distribution

$$P(z) = (P_c - P_m).V(z) + P_m - \frac{\alpha}{2}(P_c + P_m) \tag{4}$$

Uneven distribution

$$P(z) = (P_c - P_m).V(z) + P_m - \frac{\alpha}{2}(P_c + P_m)(2\frac{z}{h}) \tag{5}$$

$$P(z) = (P_c - P_m).V(z) + P_m - \frac{\alpha}{2}(P_c + P_m)(1 - \frac{2|z|}{h}) \tag{6}$$

$$P(z) = (P_c - P_m).V(z) + P_m - \frac{\alpha}{2}(P_c + P_m)(\frac{1}{2} - \frac{z}{h}) \tag{7}$$

2.2 Theory and formulations

The axial displacement, u_x, and the transverse displacement of any point of the beam, u_z, are given as:

$$\begin{aligned} u(x,z,t) &= U + z(\psi_0 w' + \psi_1 \phi) + \psi_3(-zw' + f\phi) \\ w(x,z,t) &= W \end{aligned} \tag{8}$$

where "f" is the transverse shear function and $U = U(x,t)$ and $W = W(x,t)$ present denote the axial and transverse displacement of the beam at any point x and z directions while $\phi = \phi(x,t)$ is the rotational angle of the cross-section abouty-axis compared to the undeform position. The prime (') expresses the derivatives of the functions in accordance with x coordinate.

$\psi_0 = -1$, $\psi_1 = 1$ and $\psi_3 = 1$ are the constants characterizing the axial displacements over the thickness, which can be utilized to determine the shear deformation theory considered. ψ_0, ψ_1 and ψ_3 only exist in the formulations for the CBT, FOBT and HOBT. Respectively. By utilizing these constants, one can describe the CBT, FOBT and HOBT at the same time.

The strain–displacement relations are given by:

$$\varepsilon_x = \frac{\partial u}{\partial x} = U' + z[(\psi_0 - \psi_3)W'' + \psi_1\phi'] + \psi_3 f\phi' \tag{9a}$$

$$\gamma_{xz} = \frac{\partial u}{\partial z} + \frac{\partial w}{\partial x} = (1 + \psi_0 - \psi_3)W' + (\psi_1 + \psi_3\frac{df}{dz})\phi \tag{9b}$$

2.3 Variation formulation

The strain energy and kinetic energy of the FGM beam are given as:

$$\int (\delta\Pi - \delta K)dt = 0 \tag{10}$$

where $\delta\Pi$ and δK denote the virtual variation of the strain energy and kinetic energy.

The virtual variation of the strain energy is given by:

$$\delta\prod = \int_0^L \int_0^b \left[\int_{h_{n1}}^{h_n} (\sigma_x \delta\varepsilon_x + \sigma_{xz}\delta\gamma_{xz}) dz dy dx \right] \quad (11a)$$

$$\delta\prod = \int_0^L \begin{Bmatrix} N_x \delta U' + M_x \begin{bmatrix} (\psi_0 - \psi_3)\delta W'' \\ + + \psi_1 \delta\phi' \end{bmatrix} + P_x \psi_3 \delta\phi' \\ + Q_{xz}[(1 + \psi_0 - \psi_3)\delta w' + (\psi_1 + \frac{df}{dz}\psi_3)\delta\phi] \end{Bmatrix} dx \quad (11b)$$

In which:

$$N_x = \int_{\frac{-h}{2}}^{\frac{h}{2}} \sigma_x b dz \; M_x = \int_{-\frac{h}{2}}^{\frac{h}{2}} \sigma_x z b dz \quad (12a)$$

$$P_x = \int_{-\frac{h}{2}}^{\frac{h}{2}} \sigma_x f b dz \; Q_{xz} = \int_{-\frac{h}{2}}^{\frac{h}{2}} \sigma_{xz}(\psi_1 + \frac{df}{dz}\psi_3) b dz \quad (12b)$$

The virtual variation of the kinetic energy can be determined as:

$$\begin{aligned} \delta K &= \int_0^t \int_0^L (\ddot{u}\delta u + \ddot{w}\delta w)\rho(z) dx dt \; \int_0^t \int_0^L \Big\{ I_0 \begin{pmatrix} \ddot{U}\delta U \\ + \ddot{W}\delta W \end{pmatrix} \\ &= \psi_0 \big(\ddot{W}'\delta U + \ddot{U}\delta W' \big) \\ &+ + I_1 \begin{bmatrix} \\ + \psi_1 \big(\ddot{\phi}_x \delta U + \ddot{U}\delta\phi_x \big) - \psi_3 \big(\ddot{W}'\delta U + \ddot{U}\delta W' \big) \end{bmatrix} \\ &+ + I_2 \big(-\psi_0 \ddot{W}'\delta W' + \psi_1 \ddot{\phi}_x \delta\phi_x + \psi_3 \ddot{W}'\delta W' \big) \\ &+ I_f \psi_3 \big(\ddot{\phi}_x \delta U + \ddot{U}\delta\phi_x \big) - I_{zf}\psi_3 \big(\ddot{\phi}_x \delta W' + \ddot{W}'\delta\phi_x \big) \\ &+ I_{f^2}\psi_3 \ddot{\phi}_x \delta\phi_x \Big\} dx dt \end{aligned} \quad (13)$$

where:

$$(I_0, I_1, I_2, I_f, I_{fz}, I_{f^2}) = \int_{-\frac{h}{2}}^{\frac{h}{2}} (1, z, z^2, f, zf, f^2)\rho(z) b dz \quad (14)$$

2.4 Constitutive equations

The stress–strain relation for the FGM beam is expressed as:

$$\begin{aligned} \sigma_x &= E\varepsilon_x \\ \sigma_{xz} &= \frac{E}{2[1+\nu]}\gamma_{xz} \end{aligned} \quad (15)$$

By subbing Eq. (6) into Eq. (12), the stress resultants can be extended as below:

$$\begin{Bmatrix} N_x \\ M_x \\ P_x \\ Q_{xz} \end{Bmatrix} = \begin{bmatrix} A & B & C & 0 \\ B & D & F & 0 \\ C & F & H & 0 \\ 0 & 0 & 0 & A_s \end{bmatrix} \begin{Bmatrix} U' \\ (\psi_0 - \psi_3)W'' + \psi_1\phi' \\ \psi_3\phi' \\ (1 + \psi_0 - \psi_3)W' + (\psi_1 + \psi_3)\phi \end{Bmatrix} \quad (16)$$

where:

$$(A, B, D, C, F, H) = \int_A E(1, z, z^2, f, zf, f^2) dA \quad (17)$$

$$A_s = \int_A \frac{E}{2(1+\upsilon)} \left[\psi_1 + \psi_3 (\frac{df}{dz})^2 \right] dA \quad (18)$$

2.5 Governing equations of motion

By substituting Eqs. (11) and (13) into Eq. (10), integrating the equation by part, and collecting the coefficients of δU, $\delta\phi$ and δW the general equation of vibration of FG beam can be written as:

$$N_x' = I_0 \ddot{U} + I_1 (\psi_0 \ddot{W}' + \psi_1 \ddot{\phi} - \psi_3 \ddot{W}'^{3f} \quad (19a)$$

$$\begin{aligned} M_x''(\psi_3 - \psi_0) &= I_0 \ddot{W} - I_1 \big(\psi_0 \ddot{U}' - \psi_3 \ddot{U}' \big) \\ &+ I_2 (\psi_0 \ddot{W}'' - \psi_3 \ddot{W}'') + \psi_3 I_{zf} \ddot{\phi}' \end{aligned} \quad (19b)$$

$$\begin{aligned} &M_x' \psi_1 + P_x' \psi_3 - Q_{xz}(\psi_1 + \psi_3) \\ &= I_1\psi_1\ddot{U} + I_2\psi_1\ddot{\phi} + I_f\psi_3\ddot{U} - I_{zf}\psi_3\ddot{W}' + I_{f^2}\psi_3\ddot{\phi} \end{aligned} \quad (19c)$$

By using the state space approach, the displacement components can be expressed as:

$$\begin{Bmatrix} U(x,t) \\ \phi(x,t) \\ W(x,t) \end{Bmatrix} = \begin{bmatrix} U(x) \\ \phi(x) \\ W(x) \end{bmatrix} e^{i\omega t} \quad (20)$$

where ω is the eigen-frequency, which we point out that this assumption has been made.

By substituting Eq. (20) into Eq. (19), a system of ordinary differential equations is obtained:

$$\textbf{For CBT:} \begin{cases} U'' = e_1 U + e_2 W' + e_3 W''' \\ W^{iv} = e_4 U' + e_5 W + e_6 W'' \end{cases} \quad (21)$$

$$\textbf{For FOBT:} \begin{cases} U'' = c_1 U + c_2 \phi + c_3 W' \\ \phi'' = c_4 U + c_5 \phi + c_6 W' \\ W'' = c_7 \phi' + c_8 W \end{cases} \quad (22)$$

$$\textbf{For HOBT:} \begin{cases} U'' = b_1 U + b_2 \phi + b_3 W + b_4 W''' \\ \phi'' = b_5 U + b_6 \phi + b_7 W' + b_8 W'' \\ W^{iv} = b_9 U' + b_{10}\phi' + b_{11} W + b_{12} W'' \end{cases} \quad (23)$$

where the e_n, c_n and b_n are the constants coefficients and are described in the Appendix.

The systems of Eqs. (21)-(23) can be converted into a matrix form as:

$$Z'(x) = TZ(x) \quad (24)$$

where:

$$Z(x) = \{U, U', W, W', W'', W'''\} \text{ for CBT.} \quad (25a)$$

$$Z(x) = \{U, U', \phi, \phi', W, W''\} \text{ for FOBT.} \quad (25b)$$

$$Z(x) = \{U, U', \phi, \phi', W, W', W'', W'''\} \text{ for HOBT.} \quad (25c)$$

And matrix T can be seen in the Appendix.

A formal solution of Eq. (24) is given by:

$$Z(x) = e^{Tx}K \quad (26a)$$

where K is a constant column vector determined from the boundary conditions at $x = \pm L/2$; and e^{Tx} is the general matrix solution of Eq. (24) which is given as:

$$e^{Tx} = [E]\begin{bmatrix} e^{\lambda_1 x} & & 0 \\ & \ddots & \\ 0 & & e^{\lambda_n x} \end{bmatrix}[E]^{-1} \quad (26b)$$

where $\lambda_i (i = \overline{1,n} = \overline{1,6})$ for CBT and FOBT, $\lambda_i (i = \overline{1,n} = \overline{1,8})$ for HOBT and $[E]$ are eigenvalues and corresponding matrix of eigenvectors, respectively, associated with the matrix T.

2.6 Boundary conditions (BCs)

In this paper a classical boundary conditions are investigated. Boundary conditions can be expressed in terms of unknown function $Z(x)$ as follows:

For CBT:

$$\text{Clamped (C):}\ U = W = W' = 0 \quad (27a)$$

$$\text{Hinged (H):}\ U = W = BU' - DW'' = 0 \quad (27b)$$

$$\text{Pinned (P):}\ AU' - BW'' = W = BU' - DW'' = 0 \quad (27c)$$

$$\text{Free (F):}\ AU' - BW'' = BU' - DW'' = BU'' - DW''' + I_1\omega^2 U - I_2\omega^2 W' = 0 \quad (27d)$$

For FOBT:

$$\text{Clamped (C):}\ U = \phi = W = 0 \quad (28a)$$

$$\text{Hinged (H):}\ U = W = BU'' + D\phi' = 0 \quad (28b)$$

$$\text{Pinned (P):}\ AU' + B\phi' = W = BU' + D\phi' = 0 \quad (28c)$$

$$\text{Free (F):}\ AU' + B\phi' = BU' + D\phi' = A_s(\phi + W') = 0 \quad (28d)$$

For HOBT:

$$\text{Clamped (C):}\ U = \phi = W = W' = 0 \quad (29a)$$

$$\text{Hinged (H):}\ U = W = AU' - FW'' + H\phi' = BU' - DW'' + F\phi' = 0 \quad (29b)$$

$$\text{Pinned (P):}\ AU' - BW'' + C\phi' = W = AU' - FW'' + H\phi' = BU' - DW'' + F\phi' = 0 \quad (29c)$$

$$\text{Free (F):}\ AU' - BW'' + C\phi' = BU' - DW'' + F\phi' = BU'' - DW''' + F\phi'' + I_1\omega^2 U + J_2\omega^2\phi - I_2\omega^2 W' = AU' - FW'' + H\phi' = 0 \quad (29d)$$

Substituting Eq. (24) into Eqs. (27)-(29), a homogeneous system of equations is obtained as:

$G_{ij} \rightleftarrows K_i = 0,\ (i,j) = \overline{1,n} = \overline{1,6}$ for CBT, FOBT and $(i,j) = \overline{1,n} = 8$ for HOBT.

where

$$[G(x)] = [E]\begin{bmatrix} e^{\lambda_1 x} & & 0 \\ & \ddots & \\ 0 & & e^{\lambda_n x} \end{bmatrix}[E]^{-1} \quad (30)$$

By setting the determinant of G_{ij} to zero, the natural frequency ω can be determined. It should be noted that a trial and error procedure need to be used to obtain the natural frequency values due to the attendant of unknown ω in matrix T.

3. Results and discussion:

Numerical investigation is carried out in this section to show the efficiency of the present approach and to illustrate the effects of various parameters on the free vibration behavior of the porous PFGM and SFGM beams. Otherwise stated, The FG beam made from aluminum (Al) and alumina (Al_2O_3) with the following material properties is employed here with:

- Em = 70 GPa, ρm = 2702 kg/m^3, νm = 0.3 for aluminum.
- Ec = 380 GPa, ρc = 3960 kg/m^3, νc = 0.3 for alumina.

Table 1 shows the comparison of fundamental non-dimensional frequencies of perfect FG beams with various. The material parameters are 0, 1, 2, 5 and 10. All the results relating to PFGM and SFGM beams under C–C, C–F and S–S boundary conditions agree well with Sayyad *et al* (2018) for perfect FG beams. It can be seen that natural frequencies reduce significantly along with the increase of gradient index k.

Tables 2 and 3 provide the effect of volume fraction of porosity on the fundamental non-dimensional frequencies of imperfect FG beams with various boundary conditions. The volume fraction of porosity is taken equal 0.1 and 0.2. The span-to-depth ratio is taken equal to L/h = 5. It is seen that for an imperfect FG beams the fundamental non-dimensional frequencies become more important.

The influence of porosity on the fundamental non-dimensional frequencies of a perfect and imperfect FG beams with span-to-depth ratio equal to 20 is also presented in the Tables 4-6. The results are calculated with five values of gradient index (k = 0, 1, 2, 5 and 10). As expected, the results from imperfect FG beams are larger than perfect beams due to decrement of beam's stiffness. The inclusion of porosity effect leads to increase fundamental non-dimensional frequencies.

The effect of span to depth ratio (L/h) on the fundamental non-dimensional frequencies of FG beams is shown in Table 7. The effect of the volume porosity fraction is also presented in both law of mixture models. It can be seen that the results are in excellent agreement with those

Table 1 Comparison of the fundamental non-dimensional frequencies of FG beams for different boundary conditions Alpha = 0, L/h = 5t

Theory	k	PFGM			SFGM		
		CC	CF	SS	CC	CF	SS
CBT	0	12.1826 12.1826*	1.9385 1.93845*	5.3953 5.39530*	10.2214 -	1.6265 -	4.5267 -
	1	9.3642 9.36422*	1.4914 1.49135*	4.1484 4.14840*	9.3642 -	1.4914 -	4.1484 -
	2	8.5277 8.52772*	1.3599 1.35985*	3.7793 3.77930*	8.8483 -	1.4099 -	3.9204 -
	5	8.1096 8.10955*	1.2942 1.29416*	3.5949 3.59490*	8.3861 -	1.3368 -	3.7162 -
	10	7.8797 7.87968*	1.2565 1.25648*	3.4921 3.49210*	8.2447 -	1.3144 -	3.6536 -
FBT	0	9.9975 10.0344*	1.8944 1.89479*	5.1525 5.15247*	8.3879 -	1.5894 -	4.3229 -
	1	7.8998 7.92529*	1.4628 1.46300*	3.9903 3.99023*	7.8998 -	1.4628 -	3.9903 -
	2	7.1880 7.21134*	1.3335 1.33376*	3.6344 3.63438*	7.5854 -	1.3857 -	3.7864 -
	5	6.6428 6.66764*	1.2642 1.26445*	3.4312 3.43119*	7.2904 -	1.3161 -	3.6015 -
	10	6.3148 6.34062*	1.2237 1.22398*	3.3135 3.31343*	7.1975 -	1.2948 -	3.5445 -
HBT	0	10.0723 10.0847*	1.8953 1.89630*	5.1529 5.15423*	8.4504 -	1.5901 -	4.3233 -
	1	7.9514 7.95826*	1.4633 1.45116*	3.9905 3.99140*	7.9514 -	1.4633 -	3.9905 -
	2	7.1769 7.19737*	1.3326 1.32138*	3.6263 3.62671*	7.6427 -	1.3864 -	3.7881 -
	5	6.4900 6.50354*	1.2590 1.25892*	3.4003 3.40000*	7.3603 -	1.3172 -	3.6055 -
	10	6.1651 6.19012*	1.2183 1.22589*	3.2812 3.28135*	7.2728 -	1.2960 -	3.5494 -

*Sayyad *et al*. (2018)

Table 2 Comparison of the fundamental non-dimensional frequencies of FG beams for different boundary conditions Alpha = 0.1; L/h = 5

Theory	k	PFGM			SFGM		
		CC	CF	SS	CC	CF	SS
CBT	0	12.3472	1.9646	5.4682	10.2214	1.6264	4.5267
	1	9.1526	1.4579	4.0548	9.1526	1.4579	4.0548
	2	8.0671	1.2873	3.5760	8.4963	1.3542	3.7649
	5	7.4911	1.1971	3.3222	7.8980	1.2595	3.5003
	10	7.2927	1.1644	3.2333	7.7125	1.2301	3.4183
FBT	0	10.1325	1.9200	5.2221	8.3879	1.5894	4.3229
	1	7.7726	1.4312	3.9069	7.7726	1.4312	3.9069
	2	6.8841	1.2643	3.4496	7.3619	1.3328	3.6458
	5	6.2154	1.1713	3.1816	6.9648	1.2422	3.4041
	10	5.8688	1.1346	3.0713	6.8373	1.2140	3.3285
HBT	0	10.2081	1.9209	5.2225	8.4504	1.5901	4.3233
	1	7.8218	1.4317	3.9071	7.8218	1.4317	3.9071
	2	6.8685	1.2633	3.4417	7.4176	1.3335	3.6478
	5	6.0268	1.1653	3.1468	7.0352	1.2433	3.40874
	10	5.6496	1.1271	3.0285	6.9142	1.2152	3.3342

Table 3 Comparison of the fundamental non-dimensional frequencies of FG beams for different boundary conditions Alpha = 0,2; L/h = 5

Theory	k	PFGM			SFGM		
		CC	CF	SS	CC	CF	SS
CBT	0	12.5421	1.9957	5.5545	10.2212	1.6264	4.5267
	1	8.8483	1.4099	3.9204	8.8483	1.4099	3.9204
	2	7.3395	1.1724	3.2545	7.9796	1.2725	3.5364
	5	6.3705	1.0208	2.8275	7.1625	1.1429	3.1749
	10	6.1994	0.9930	2.7514	6.9030	1.1017	3.0601
FBT	0	10.2925	1.9503	5.3045	8.3879	1.5894	4.3229
	1	7.5854	1.3857	3.7864	7.5854	1.3857	3.7864
	2	6.3926	1.1544	3.1554	7.0202	1.2546	3.4373
	5	5.4525	1.0027	2.7295	6.4472	1.1299	3.1027
	10	5.0958	0.9702	2.6284	6.2567	1.0901	2.9953
HBT	0	10.3693	1.9512	5.3050	8.45049	1.5901	4.3233
	1	7.6309	1.3862	3.7866	7.6309	1.3862	3.7866
	2	6.3766	1.1535	3.1488	7.2653	1.2553	3.4396
	5	5.2423	0.9967	2.6950	6.8094	1.1311	3.1080
	10	4.7672	0.9597	2.5704	6.3341	1.0914	3.0017

Table 4 Comparison of the fundamental non-dimensional frequencies of FG beams for different boundary conditions Alpha = 0; L/h = 20

Theory	k	PFGM			SFGM		
		CC	CF	SS	CC	CF	SS
CBT	0	12.4143	1.9525	5.4778	10.4156	1.6381	4.5958
	1	9.5554	1.5030	4.2164	9.5554	1.5030	4.2164
	2	8.7186	1.3714	3.8472	9.0359	1.4213	3.9871
	5	8.3007	1.3058	3.6629	8.5694	1.3479	3.7813
	10	8.0556	1.2672	3.5547	8.4264	1.3255	3.7183
FBT	0	12.2202	1.9496	5.4603	10.2527	1.6357	4.5812
	1	9.4292	1.5010	4.2051	9.4292	1.5010	4.2051
	2	8.6020	1.3697	3.8368	8.9290	1.4197	3.9776
	5	8.1676	1.3038	3.6509	8.4778	1.3466	3.7732
	10	7.9102	1.2650	3.5416	8.3395	1.3242	3.7105
HBT	0	12.2222	1.9496	5.4604	10.2544	1.6357	4.5812
	1	9.4306	1.5011	4.2051	9.4306	1.5011	4.2051
	2	8.5964	1.3696	3.8362	8.9313	1.4197	3.9777
	5	8.1426	1.3034	3.6484	8.4820	1.3466	3.7735
	10	7.8846	1.2645	3.5390	8.3441	1.3242	3.7109

Table 5 Comparison of the fundamental non-dimensional frequencies of FG beams for different boundary conditions Alpha = 0.10; L/h = 20

Theory	k	PFGM			SFGM		
		CC	CF	SS	CC	CF	SS
CBT	0	12.5820	1.9789	5.5518	10.4156	1.6381	4.5958
	1	9.3423	1.4694	4.1223	9.3423	1.4694	4.1223
	2	8.2561	1.2987	3.6432	8.6806	1.3654	3.8304

Table 5 Continued

Theory	k	PFGM			SFGM		
		CC	CF	SS	CC	CF	SS
CBT	5	7.6835	1.2088	3.3906	8.0757	1.2703	3.5635
	10	7.4699	1.1751	3.2963	7.8878	1.2408	3.4806
FBT	0	12.3852	1.9759	5.5341	10.2527	1.6357	4.5812
	1	9.2242	1.4677	4.1118	9.2242	1.4677	4.1118
	2	8.1544	1.2972	3.6341	8.5857	1.3640	3.8219
	5	7.5687	1.2070	3.3803	7.9991	1.2692	3.5567
	10	7.3372	1.1731	3.2843	7.8164	1.2397	3.4743
HBT	0	12.3875	1.9759	5.5341	10.2544	1.6357	4.5812
	1	9.2255	1.4677	4.1118	9.2255	1.4677	4.1118
	2	8.1488	1.2971	3.6335	8.5882	1.3640	3.8221
	5	7.5401	1.2066	3.3776	8.0034	1.2692	3.5570
	10	7.3017	1.1725	3.2809	7.8214	1.2398	3.4747

Table 6 Comparison of the fundamental non-dimensional frequencies of FG beams for different boundary conditions Alpha = 0. 20; L/h = 20

Theory	k	PFGM			SFGM		
		CC	CF	SS	CC	CF	SS
CBT	0	12.7806	2.0101	5.6394	10.4156	1.6381	4.5958
	1	9.0359	1.4213	3.9871	9.0359	1.4213	3.9871
	2	7.5235	1.1836	3.3200	8.1582	1.2833	3.6000
	5	6.5612	1.0324	2.8955	7.3301	1.1531	3.2346
	10	6.3811	1.0040	2.8160	7.0665	1.1116	3.1183
FBT	0	12.5808	2.0071	5.6215	10.2527	1.6357	4.5812
	1	8.9290	1.4197	3.9776	8.9290	1.4197	3.9776
	2	7.4437	1.1824	3.3128	8.0794	1.2821	3.5929
	5	6.4804	1.0312	2.8883	7.2727	1.1522	3.2295
	10	6.2790	1.0025	2.8069	7.0151	1.1109	3.1137
HBT	0	12.5836	2.0071	5.6215	10.2544	1.6357	4.5812
	1	8.9301	1.4197	3.9776	8.9301	1.4197	3.9776
	2	7.4388	1.1823	3.3123	8.0819	1.2822	3.5931
	5	6.4516	1.0307	2.8856	7.2773	1.1523	3.2298
	10	12.7806	2.0101	5.6394	10.4156	1.6381	4.5958

Table 7 The fundamental non-dimensional frequencies of FG beams with respect to span to depth ratio

alpha	1/h	PFGM			SFGM		
		CC	CF	SS	CC	CF	SS
0	5	7.1770	1.3326	3.6263 $3.642^{(1)}$	7.6426	1.3864	3.7881 $3.793^{(1)}$
	10	8.2329	1.3618	3.7905 $3.795^{(1)}$	8.6109	1.4128	3.9369 $3.938^{(1)}$
	20	8.5964	1.3696	3.8362 $3.837^{(1)}$	8.9313	1.4197	3.9777 $3.978^{(1)}$
	50	8.7095	1.3718	3.8493 $3.85^{(1)}$	9.0295	1.4217	3.9895 $3.989^{(1)}$
	100	8.7262	1.3721	3.8512 $3.851^{(1)}$	9.0439	1.4220	3.9912 $3.991^{(1)}$

Table 7 Continued

alpha	1/h	PFGM			SFGM		
		CC	CF	SS	CC	CF	SS
0.20	5	6.3766	1.1535	3.1488 3.174(1)	7.0736	1.2553	3.4396 3.452(1)
	10	7.1738	1.1763	3.2769 3.284(1)	7.8372	1.2766	3.5602 3.564(1)
	20	7.438799	1.1823	3.3123 3.314(1)	8.0819	1.2822	3.5931 3.594(1)
	50	7.5202	1.1840	3.3225 3.323(1)	8.1561	1.2837	3.6025 3.603(1)
	100	7.5322	1.1842	3.3240 3.324(1)	8.1669	1.2840	3.6039 3.604(1)

(1)Avcar 2019

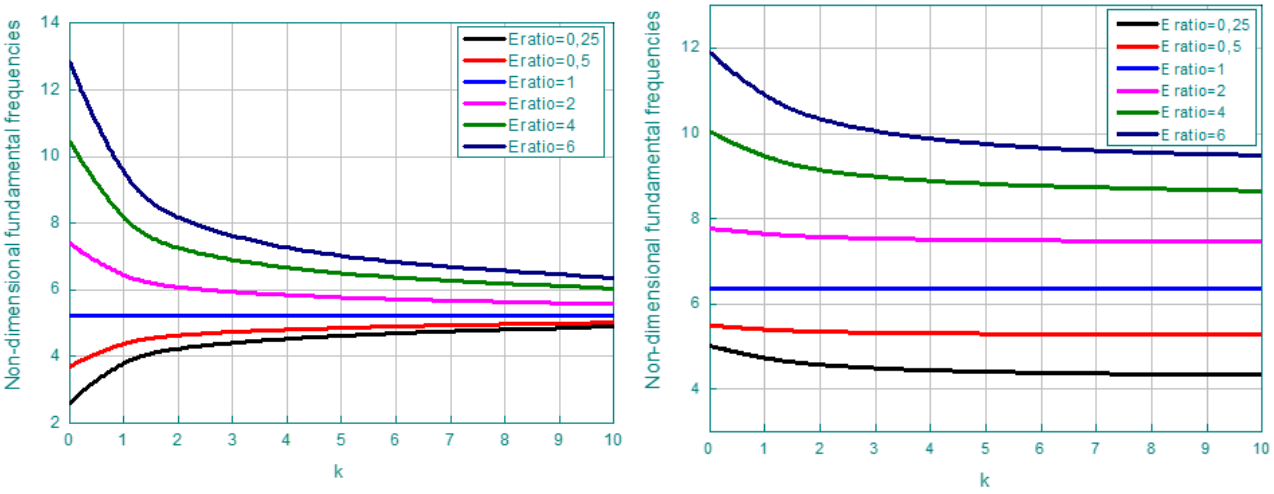

PFGM beam SFGM beam

Fig. 1 Effect of Young's modulus ratio on the non-dimensional fundamental natural frequencies of clamped-clamped FGM beam with respect to power-law exponent (L/h = 5)

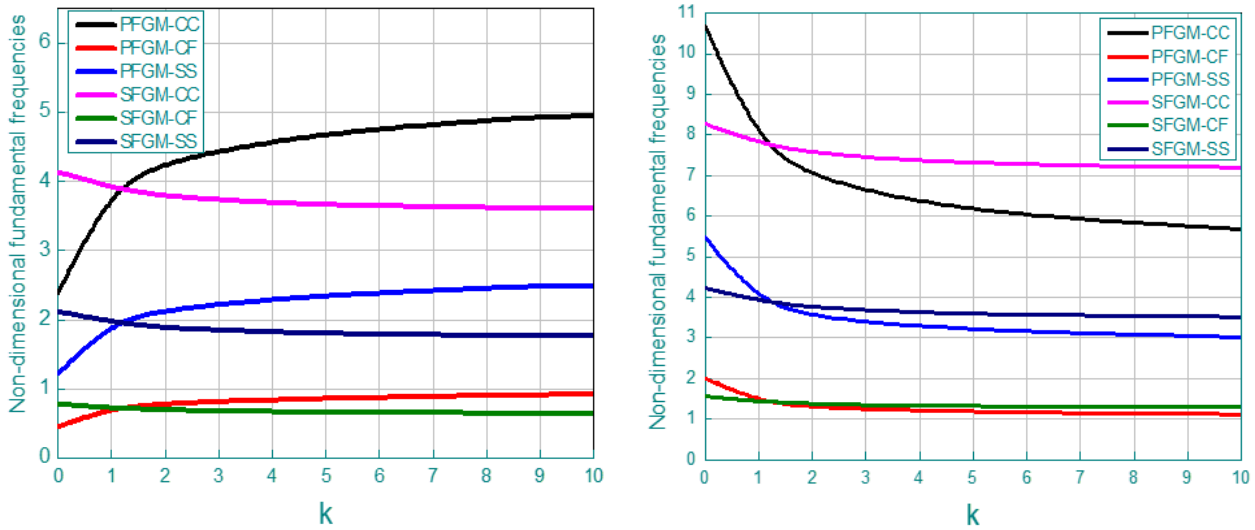

Eratio = 0.25 Eratio = 4

Fig. 2 Effect of the boundary conditions on the non-dimensional fundamental natural frequencies of FG beam with respect to power-law exponent (l/h = 5)

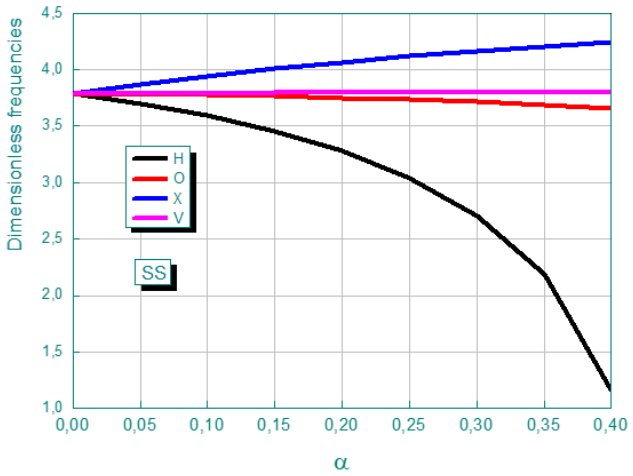

PFGM beam

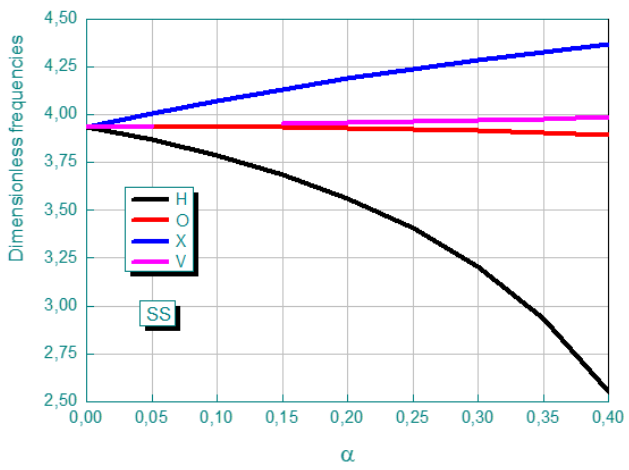

SFGM beam

Fig. 3 The variation of the dimensionless fundamental frequency of porous FGM beam versus porosity volume fraction

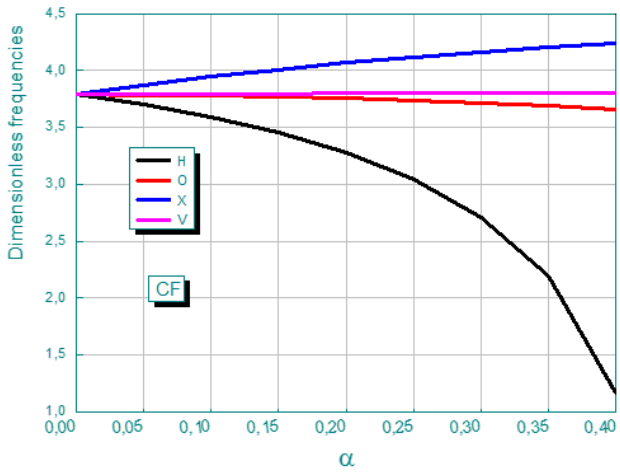

PFGM beam

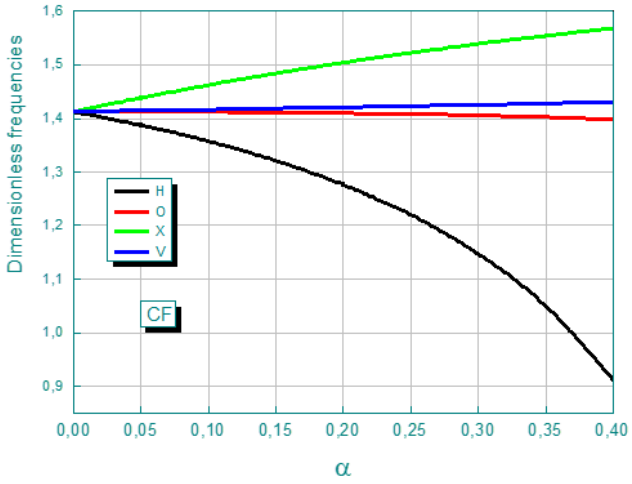

SFGM beam

Fig. 4 The variation of the dimensionless fundamental frequency of porous FGM beam versus porosity volume fraction

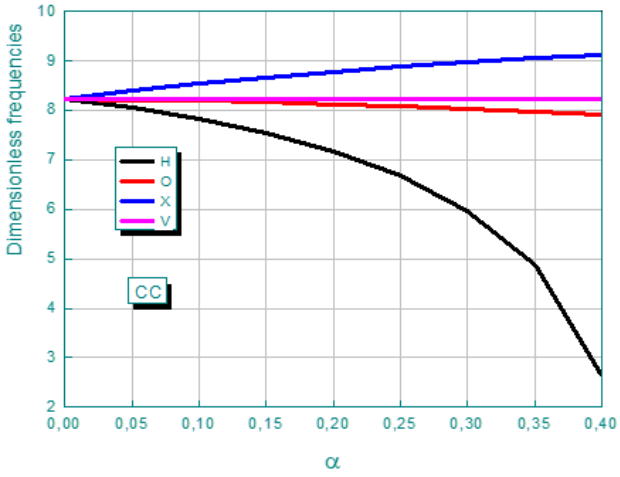

PFGM beam

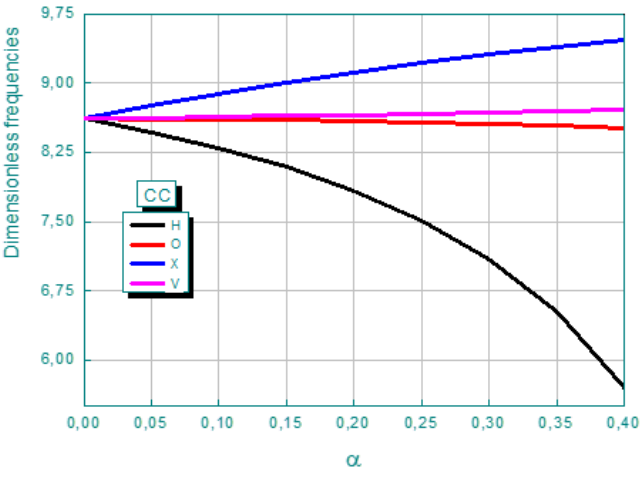

SFGM beam

Fig. 5 The variation of the dimensionless fundamental frequency of clamped-clamped porous FGM beam versus porosity volume fraction

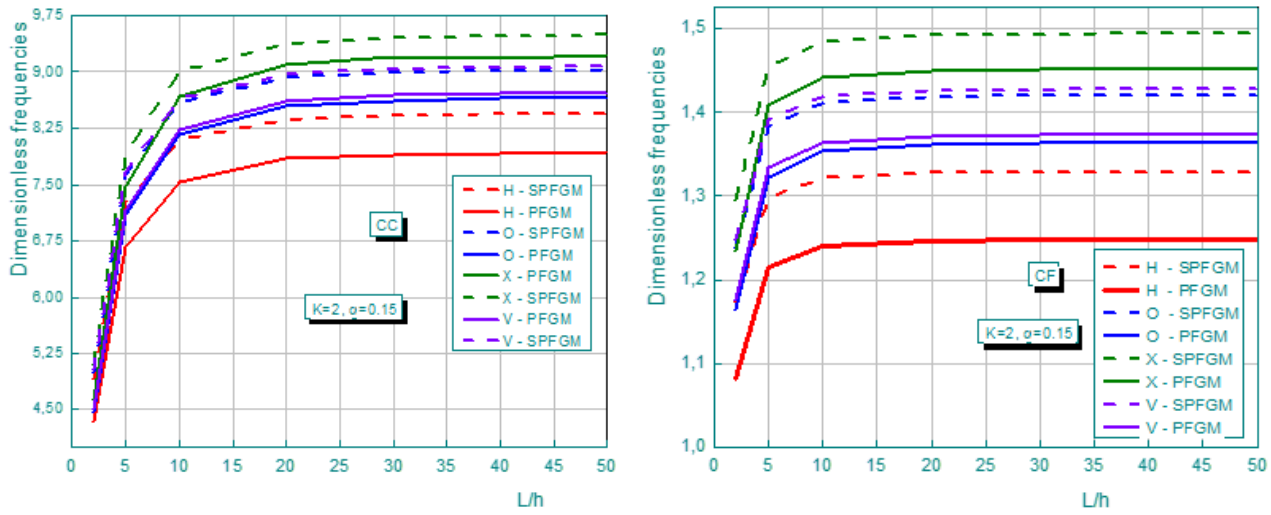

CC CF

Fig. 6 The variation of the dimensionless fundamental frequency of porous FG beam versus span-to-depth ratio

from of Avcar (2019). Also, the fundamental non-dimensional frequencies increase with increasing of span to depth ratio (L/h) and decreases when the beam contains pores.

Fig 1. present the effect of Young's modulus ratio on the non-dimensional fundamental natural frequencies of clamped-clamped FGM beam versus gradient index (k). The span-to-depth ratio is taken equal to L/h = 5. Two forms of mixing laws are used namely PFGM and SFGM. This figure showed that the values of non-dimensional fundamental natural frequencies decrease with the increase of Young's modulus ratio for both perfect PFGM and SFGM beams.

The effect of the boundary conditions on the non-dimensional fundamental natural frequencies of FG beam versus power-law exponent is shown in Fig 2. The value of Young's modulus ratio is taken equal Eratio = 0.25 and 4. It can be seen that the non-dimensional fundamental natural frequencies become more important with the increase of the Young's modulus ratio.

The Figs. 3-5 show the effect of the distribution shape of the porosity on the dimensionless fundamental frequency of imperfect FGM beam under various boundary conditions versus porosity volume fraction. Different distribution shapes of porosity are taken into consideration, namely: homogenous, O, X and V shapes. From these figures, it can be seen that the effect of the distribution shape of porosity on the dimensionless fundamental frequency becomes more important with the increase in the volume fraction of porosity for different boundary conditions.

The variation of the dimensionless fundamental frequency of porous FG beam as a function of span-to-depth ratio (L/h) is presented in Fig. 6. The gradient index is taken equal k = 2 and the volume fraction of porosity is a = 0.15. Two types of law of mixture are used in these figures namely: PFGM and SFGM. As can be seen, by increase in the span-to-depth ratio, the dimensionless fundamental frequency of porous FG beam increase in all porosities models.

4. Conclusions

In the present article, dynamic analyses of functionally graded beams are investigated using state-space approach. The FG beams are considered with porosities and the materials are assumed to be graded in the thickness direction according to PFGM and SFGM distribution. The equations of motion and the boundary conditions are derived by using the Hamilton's principle. The effect of various boundary conditions, power law index, span-to-depth ratios, porosity and its distribution shape on the free vibration frequency of the FG beams are discussed. According of the present study, the following conclusion can be drawn:

• The results obtained for the fundamental frequencies by the present approach agree well with the reference solutions considered.

• More metal content in the FG beam causes lower fundamental frequencies, on the other hand more porosity content in the FG beam causes greater fundamental frequencies.

• The variation of the distribution shape of porosity in the FG beam has an important effect on the fundamental frequencies.

References

Abdulrazzaq, M.A., Fenjan, R.M., Ahmed, R.A. and Faleh, N.M. (2020), "Thermal buckling of nonlocal clamped exponentially graded plate according to a secant function based refined theory", *Steel Compos. Struct.*, **35**(1), 147-157. http://doi.org/10.12989/scs.2020.35.1.147.

Abdelhak, Z., Hadji, L., Daouadji, T.H. and Adda Bedia, E.A. (2016), "Thermal buckling response of functionally graded sandwich plates with clamped boundary conditions", *Smart Struct. Syst.*, **18**(2), 267-291. https://doi.org/10.12989/sss.2016.18.2.267.

Abderezak, R., Daouadji, T.H. and Rabia, B. (2021), "Modeling and analysis of the imperfect FGM-damaged RC hybrid

beams", *Adv. Comput. Des.*, **6**(2), 117-133. http://doi.org/10.12989/acd.2021.6.2.117.

Aicha, K., Rabia, B., Daouadji, T.H. and Bouzidene, A. (2020), "Effect of porosity distribution rate for bending analysis of imperfect FGM plates resting on Winkler-Pasternak foundations under various boundary conditions", *Coupled Syst. Mech.*, **9**(6), 575-597. http://doi.org/10.12989/csm.2020.9.6.575.

Allahkarami, F. (2020), "Dynamic buckling of functionally graded multilayer graphene nanocomposite annular plate under different boundary conditions in thermal environment", *Eng. Comput.*, 1-24. https://doi.org/10.1007/s00366-020-01169-7.

Anwariningsih, S.H. (2013), "Development of interactive media for ict learning at elementary school based on student self learning", *J. Educ. Learn*, **7**(154), 121-128. https://doi.org/10.11591/edulearn.v7i2.226.

Arefi, M. and Zur, K.K. (2020), "Free vibration analysis of functionally graded cylindrical nanoshells resting on Pasternak foundation based on two-dimensional analysis", *Steel Compos. Struct.*, **34**(4), 615-623. http://doi.org/10.12989/scs.2020.34.4.615.

Ashraf, M.A., Liu, Z., Zhang, D., Pham, B.T. (2020), "Effects of elastic foundation on the large-amplitude vibration analysis of functionally graded GPL-RC annular sector plates", *Eng. Comput.*, 1-21. https://doi.org/10.1007/s00366-020-01068-x.

Asrari, R., Ebrahimi, F. and Kheirikhah, M. M. (2020), "On post-buckling characteristics of functionally graded smart magneto-electro-elastic nanoscale shells" *Adv. Nano Res.*, **9**(1), 33-45. http://doi.org/10.12989/anr.2020.9.1.033.

Avcar, M. (2019), "Free vibration of imperfect sigmoid and power law functionally graded beams", *Steel Compos. Struct.*, **30**(6), 603-615. http://doi.org/10.12989/scs.2019.30.6.603.

Benferhat, R., Hassaine, D.T., Said, M.M., and Hadji, L. (2016), "Effect of porosity on the bending and free vibration response of functionally graded plates resting on Winkler-Pasternak foundations", *Earthq. Struct.*, **10**(6), 1429-1449. https://doi.org/10.12989/eas.2016.10.6.1429.

Benferhat, R., Tahar, H.D. and Rabahi, A. (2019), "Effect of distribution shape of the porosity on the interfacial stresses of the FGM beam strengthened with FRP plate", *Earthq. Struct.*, **16**(5), 601-609. https://doi.org/10.12989/eas.2019.16.5.601.

Benferhat, R., Hassaine D.T. and Abderezak, R. (2020), "Thermo-mechanical behavior of porous FG plate resting on the Winkler-Pasternak foundation", *Coupled Syst. Mech.*, **9**(6), 499-519. http://doi.org/10.12989/csm.2020.9.6.499.

Benferhat, R., Hassaine, D.T. and Rabahi, A. (2021), "Effect of porosity on fundamental frequencies of FGM sandwich plates", *Compos. Mater. Eng.*, **3**(1), 25-40. http://doi.org/10.12989/cme.2021.3.1.025.

Eltaher, M.A. and Akbas, S.D. (2020), "Transient response of 2D functionally graded beam structure", *Struct. Eng. Mech.*, **75**(3), 357-367. http://doi.org/10.12989/sem.2020.75.3.357.

Esmaeili, M. and Beni, Y.T. (2019), "Vibration and buckling analysis of functionally graded flexoelectric smart beam", *J. Appl. Comput. Mech.*, **5**(5), 900-917. https://doi.org/10.22055/jacm.2019.27857.1439.

Ghannadpour, S.A.M. and Mehrparvar, M. (2020), "Nonlinear and post-buckling responses of FGM plates with oblique elliptical cutouts using plate assembly technique", *Steel Compos. Struct.*, **34**(2), 227-239. http://doi.org/10.12989/scs.2020.34.2.227.

Ghayesh, M.H. (2018a), "Nonlinear vibrations of axially functionally graded Timoshenko tapered beams", *J. Comput. Nonlinear Dynam.*, **13**(4), 041002. https://doi.org/10.1115/1.4039191.

Ghayesh, M.H. (2018b), "Nonlinear dynamics of multilayered microplates", *J. Comput. Nonlinear Dynam.*, **13**(2), 021006. https://doi.org/10.1115/1.4037596.

Ghayesh, M.H. (2019a), "Nonlinear oscillations of FG cantilevers", *Appl. Acoust.*, **145**, 393-398. https://doi.org/10.1016/j.apacoust.2018.08.014.

Ghayesh, M.H. (2019b), "Viscoelastic mechanics of Timoshenko functionally graded imperfect microbeams" *Compos. Struct.*, **225**(1), 110974. https://doi.org/10.1016/j.compstruct.2019.110974.

Ghayesh, M.H. (2019c), "Mechanics of viscoelastic functionally graded microcantilevers", *Eur. J. Mech. A Solid*, **73**, 492-499. https://doi.org/10.1016/j.euromechsol.2018.09.001.

Ghayesh, M.H. (2019d), "Viscoelastic dynamics of axially FG microbeams", *Int. J. Eng. Sci.*, **135**, 75-85. https://doi.org/10.1016/j.ijengsci.2018.10.005.

Hadj, B., Rabia, B. and Daouadji, T.H. (2021), "Vibration analysis of porous FGM plate resting on elastic foundations: Effect of the distribution shape of porosity", *Coupled Syst. Mech.*, **10**(1), 61-77. http://doi.org/10.12989/csm.2021.10.1.061.

Heidari, F., Afsari, A. and Janghorban, M. (2020), "Several models for bending and buckling behaviors of FG-CNTRCs with piezoelectric layers including size effects", *Adv. Nano Res.*, **9**(3), 193-210. http://doi.org/10.12989/anr.2020.9.3.193.

Henni, M.A.B., Abbes, B., Daouadji, T.H., Abbes, F. and Adim, B. (2021), "Numerical modeling of hygrothermal effect on the dynamic behavior of hybrid composite plates", *Steel Compos. Struct.*, **39**(6), 751-763. http://doi.org/10.12989/scs.2021.39.6.751.

Huang, Y., Li, X.F.A. (2010), "New approach for free vibration of axially functionally graded beams with non-uniform cross-section", *J. Sound Vib.*, **329**(11), 2291-2303. https://doi.org/10.1016/j.jsv.2009.12.029.

Karami, B., Shahsavari, D., Janghorban, M. and Li, L. (2020), "Free vibration analysis of FG nanoplate with poriferous imperfection in hygrothermal environment" *Struct. Eng. Mech.*, **73**(2), 191-207. http://doi.org/10.12989/sem.2020.73.2.191.

Koochi, A. and Goharimanesh, M., (2021), "Nonlinear oscillations of CNT nano-resonator based on nonlocal elasticity: The energy balance method", *Reports Mech. Eng.*, **2**(1), 41-50. https://doi.org/10.31181/rme200102041g.

Le, N.L., Nguyen, T.P., Vu, H.N., Nguyen, T.T. and Vu, M.D. (2020), "An analytical approach of nonlinear thermo-mechanical buckling of functionally graded graphene-reinforced composite laminated cylindrical shells under compressive axial load surrounded by elastic foundation", *J. Appl. Comput. Mech.*, **6**(2), 357-372. https://doi.org/10.22055/jacm.2019.29527.1609.

Li, L., Xiaobai, L., Yujin, H. (2016), "Free vibration analysis of nonlocal strain gradient beams made of functionally graded material", *Int. J. Eng. Sci.*, **102**, 77-92. https://doi.org/10.1016/j.ijengsci.2016.02.010.

Li, X.F. (2008), "A unified approach for analyzing static and dynamic behaviors of functionally graded Timoshenko and Euler-Bernoulli beams", *J. Sound Vib.*, **318**(4), 1210-1229. https://doi.org/10.1016/j.jsv.2008.04.056.

Liu, W.Q., Liu, S.J., Fan, M.Y., Tian, W., Wang, J. P. and Tahouneh, V (2020), "Influence of internal pores and graphene platelets on vibration of non-uniform functionally graded columns", *Steel Compos. Struct.*, **35**(2), 295-303. http://doi.org/10.12989/scs.2020.35.2.295.

Lyashenko, I.A., Borysiuk, V.N. and Popov, V.L. (2020), "Dynamical model of the asymmetric actuator of directional motion based on power-law graded materials", *Facta Univ. Series Mech. Eng.*, **18**(2), 245 - 254. https://doi.org/10.22190/FUME200129020L.

Madenci, E. and Gulcu, S. (2020), "Optimization of flexure stiffness of FGM beams via artificial neural networks by mixed FEM", *Struct. Eng. Mech.*, **75**(5), 633-642. http://doi.org/10.12989/sem.2020.75.5.633.

Mahesh, V., Harursampath, D. (2020), "Nonlinear vibration of functionally graded magneto-electro-elastic higher order plates

reinforced by CNTs using FEM", *Eng. Comput.*, 1-23. https://doi.org/10.1007/s00366-020-01098-5.

Moory-Shirbani, M., Sedighi, H.M., Ouakad, H.M. and Najar, F. (2018), "Experimental and mathematical analysis of a piezoelectrically actuated multilayered imperfect microbeam subjected to applied electric potential", *Compos. Struct.*, **184**(15), 950-960. https://doi.org/10.1016/j.compstruct.2017.10.062.

Nazemnezhad, R. and Shokrollahi, H. (2020), "Free axial vibration of cracked axially functionally graded nanoscale rods incorporating surface effect", *Steel Compos. Struct.*, **35**(3), 449-462. http://doi.org/10.12989/scs.2020.35.3.449.

Ould, L.L., Kaci, A., Houari, M.S.A., Tounsi, A. (2013), "An efficient shear deformation beam theory based on neutral surface position for bending and free vibration of functionally graded beams", *Mech. Based Des. Struct.*, **41**(4), 421-433. https://doi.org/10.1080/15397734.2013.763713.

Phung-Van, P. and Thai, C.H. A (2021), "A novel size-dependent nonlocal strain gradient isogeometric model for functionally graded carbon nanotube-reinforced composite nanoplates", *Eng. Comput.*, 1-14. https://doi.org/10.1007/s00366-021-01353-3.

Pradhan, K.K. and Chakraverty, S. (2013), "Free vibration of Euler and Timoshenko functionally graded beams by Rayleigh-Ritz method", *Compos. Part B Eng.*, **51**, 175-184. https://doi.org/10.1016/j.compositesb.2013.02.027.

Reddy, J.N. (2011), "Microstructure-dependent couple stress theories of functionally graded beams", *J. Mech. Phys. Solids*, **59**(11), 2382-2399. https://doi.org/10.1016/j.jmps.2011.06.008.

Sayyad, A.S. and Ghugal, Y.M. (2018), "Analytical solutions for bending, buckling, and vibration analyses of exponential functionally graded higher order beams", *Asian J. Civil Eng.*, **19**(5), 607-623. https://doi.org/10.1007/s42107-018-0046-z.

Sedighi, H.M., Daneshmand, F. (2014), "Static and dynamic pull-in instability of multi-walled carbon nanotube probes by He's iteration perturbation method", *J. Mech. Sci. Technol.* **28**(9), 3459-3469. https://doi.org/10.1007/s12206-014-0807-x.

Shariati, A., Mohammad-Sedighi, H., Żur, K.K., Habibi, M. and Safa, M. (2020a), "Stability and dynamics of viscoelastic moving rayleigh beams with an asymmetrical distribution of material parameters", *Symmetry*, **12**(4), 586. https://doi.org/10.3390/sym12040586.

Shariati, A., Ebrahimi, F., Karimiasl, M., Vinyas, M. and Toghroli, A. (2020b), "On transient hygrothermal vibration of embedded viscoelastic flexoelectric/piezoelectric nanobeams under magnetic loading" *Adv. Nano Res.*, **8**(1), 49-58 http://doi.org/10.12989/anr.2020.8.1.049.

Sheng, G.G., Wang, X. (2020), "Nonlinear resonance responses of size-dependent functionally graded cylindrical microshells with thermal effect and elastic medium", *Eng. Comput.*, 1-18. https://doi.org/10.1007/s00366-020-01176-8.

Şimşek, M., Kocatürk, T. (2009), "Free and forced vibration of a functionally graded beam subjected to a concentrated moving harmonic load", *Compos. Struct.*, **90**(4), 465-473. https://doi.org/10.1016/j.compstruct.2009.04.024

Şimşek, M. and Yurtcu, H.H. (2012), "Analytical solutions for bending and buckling of functionally graded nanobeams based on the nonlocal Timoshenko beam theory", *Compos. Struct.*, **97**, 378-386. https://doi.org/10.1016/j.compstruct.2012.10.038.

Simsek, M. and Reddy, J.N. (2013), "Bending and vibration of functionally graded microbeams using a new higher order beam theory and the modified couple stress theory", *Int. J. Eng. Sci.*, **64**, 37-53. https://doi.org/10.1016/j.ijengsci.2012.12.002.

Thai, H.T. and Vo, T.P. (2012), "Bending and free vibration of functionally graded beams using various higher-order shear deformation beam theories", *Int. J. Mech. Sci.*, **62**(1), 57-66. https://doi.org/10.1016/j.ijmecsci.2012.05.014.

Tlidji, Y., Benferhat, R. and Tahar, H.D. (2021), "Study and analysis of the free vibration for FGM microbeam containing various distribution shape of porosity", *Struct. Eng. Mech.*, **77**(2), 217-229. http://doi.org/10.12989/sem.2021.77.2.217.

Tran, V.K., Pham, Q.H. and Nguyen-Thoi, T. (2020), "A finite element formulation using four-unknown incorporating nonlocal theory for bending and free vibration analysis of functionally graded nanoplates resting on elastic medium foundations", *Eng. Comput.*, 1-26. https://doi.org/10.1007/s00366-020-01107-7.

Yang, F., Chong, A., Lam, D. and Tong, P. (2002), "Couple stress based strain gradient theory for elasticity", *Int. J. Solid Struct.*, **39**(10), 2731-2743. https://doi.org/10.1016/S0020-7683(02)00152-X.

Yuan, Y., Zhao, K., Zhao, Y. and Kiani, K. (2020), "Nonlocal-integro-vibro analysis of vertically aligned monolayered nonuniform FGM nanorods", *Steel Compos. Struct.*, **37**(5), 551-569. http://doi.org/10.12989/scs.2020.37.5.551.

Zhang, H., Ma, J., Ding, H. and Chen, L. (2017), "Vibration of axially moving beam supported by viscoelastic foundation", *Appl. Math. Mech.*, **38**(2), 161-172. https://doi.org/10.1007/s10483-017-2170-9.

Zhu, X., Lu, Z., Wang, Z., Xue, L. and Ebrahimi-Mamaghani, A. (2020), "Vibration of spinning functionally graded nanotubes conveying fluid", *Eng. Comput.*, 1-22. https://doi.org/10.1007/s00366-020-01123-7.

Zohra, Z.F., Lemya, H.H., Abderahman, Y., Mustapha, M., Abdelouahed, T. and Djamel, O. (2017), "Free vibration analysis of functionally graded beams using a higher-order shear deformation theory", *Math. Model. Eng. Prob.*, **4**(1)., 7-12. https://doi.org/10.18280/mmep.040102.

Zohra, A., Benferhat, R., Tahar, H.D. and Tounsi, A. (2021), "Analysis on the buckling of imperfect functionally graded sandwich plates using new modified power-law formulations", *Struct. Eng. Mech.*, **77**(6), 797-807. http://doi.org/10.12989/sem.2021.77.6.797.

JL

Appendix A. The coefficients in Eqs. (21)-(23)

For Eq. (21):

$$e_1 = \frac{-I_0\omega^2}{A},\ e_2 = \frac{-I_1\omega^2}{A},\ e_3 = \frac{B}{A},$$
$$e_4 = \frac{-(Be_1+I_1\omega^2)}{(Be_3-D)}, e_5 = \frac{-I_0\omega^2}{(Be_3-D)},\ e_6 = \frac{(I_2\omega^2-Be_2)}{(Be_3-D)}$$

For Eq. (22):

$$c_1 = \frac{(e_{2a}e_3-e_2e_{3a})}{C_0},\ c_2 = \frac{(e_{2a}e_4-e_2e_{4a})}{C_0},$$
$$c_3 = \frac{-e_2e_{5a}}{C_0},\ c_4 = \frac{(e_1e_{3a}-e_{1a}e_3)}{C_0},$$
$$c_5 = \frac{(e_1e_{4a}-e_{1a}e_4)}{C_0},\ c_6 = \frac{e_1e_{5a}}{C_0},$$
$$c_6 = \frac{-A_s}{A_s} = -1,\ c_8 = \frac{-I_0\omega^2}{A_s}$$
$$e_1 = A,\ e_2 = B,\quad e_3 = -I_0\omega^2,$$
$$e_4 = -I_1\omega^2, e_{1a} = e_2,\ e_{2a} = D,$$
$$e_{3a} = e_4,\ e_{4a} = (-I_2\omega^2 + A\ \ ),$$
$$e_{5a} = A_s\ ,\ C_0 = e_1e_{2a} - e_{1a}e_2$$

For Eq. (23):

$$b_1 = \frac{e_1e_8-e_3e_4}{e_2e_8-e_4^2},\ b_2 = \frac{e_1e_8-e_4e_7}{e_2e_8-e_4^2}, b_3 = \frac{e_5e_8-e_3e_9}{e_2e_8-e_4^2},$$
$$b_4 = \frac{-e_6e_8+e_4e_{10}}{e_2e_8-e_4^2},\ b_5 = \frac{e_2e_3-e_1e_4}{e_2e_8-e_4^2},\ b_6 = \frac{e_2e_7-e_3e_4}{e_2e_8-e_4^2},$$
$$b_7 = \frac{e_2e_9-e_4e_5}{e_2e_8-e_4^2},\ b_8 = \frac{-e_2e_{10}+e_4e_6}{e_2e_8-e_4^2}$$
$$e_1 = -I_0\omega^2,\ e_2 = A,\ e_3 = -J_1\omega^2,\ e_4 = C,$$
$$e_5 = I_1\omega^2,\ e_5 = I_1\omega^2,\ e_6 = -B,\ e_7 = K_2\omega^2 + A_s,$$
$$e_8 = H,\ e_9 = -J_2\omega^2,\ e_{10} = -F$$

Appendix B. Matrix T in Eq. (24)

For CBT:

$$\begin{bmatrix} 0 & 1 & 0 & 0 & 0 & 0 \\ e_1 & 0 & 0 & e_2 & 0 & e_3 \\ 0 & 0 & 0 & 1 & 0 & 0 \\ 0 & 0 & 0 & 0 & 1 & 0 \\ 0 & 0 & 0 & 0 & 0 & 1 \\ 0 & e_4 & e_5 & 0 & e_6 & 0 \end{bmatrix}$$

For FOBT:

$$\begin{bmatrix} 0 & 1 & 0 & 0 & 0 & 0 \\ c_1 & 0 & c_2 & 0 & 0 & c_3 \\ 0 & 0 & 0 & 1 & 0 & 0 \\ c_4 & 0 & c_5 & 0 & 0 & c_6 \\ 0 & 0 & 0 & 0 & 0 & 1 \\ 0 & 0 & 0 & c_7 & c_8 & 0 \end{bmatrix}$$